Parallel electric fields in nonlinear magnetosonic waves in an electron-positron-ion plasma

Seiichi Takahashi, Masatoshi Sato, and Yukiharu Ohsawa[a)]
Department of Physics, Nagoya University, Nagoya 464-8602, Japan

(Received 8 May 2008; accepted 28 July 2008; published online 15 August 2008)

The electric field $E_\parallel$ along the magnetic field $\boldsymbol{B}$ in nonlinear magnetosonic waves in a three-component plasma is studied with theory based on a three-fluid model and with fully kinetic, electromagnetic, particle simulations. The theory for small-amplitude ($\epsilon \ll 1$) pulses shows that the integral of $E_\parallel$ along $\boldsymbol{B}$, $F=-\int E_\parallel ds$, is proportional to $\epsilon(p_{e0}-p_{p0})$ in warm plasmas, where p_{e0} and p_{p0} are, respectively, the electron and positron pressures, and proportional to $\epsilon^2 m_i v_A^2/(1+v_A^2/c^2)^3$ in cold plasmas, where v_A is the Alfvén speed. These predictions are verified with simulations. Furthermore, for shock waves with $\epsilon \sim O(1)$, simulation values are consistent with the phenomenological relation $n_{e0}eF \sim \epsilon(\rho v_A^2+\Gamma_e p_{e0})(n_{i0}/n_{e0})$, where ρ is the mass density and Γ_e is the specific heat ratio. These results indicate that $E_\parallel$ can be strong in strong magnetic fields. © *2008 American Institute of Physics*. [DOI: 10.1063/1.2972159]

I. INTRODUCTION

In the ideal magnetohydrodynamics, the electric field parallel to the magnetic field, $E_\parallel$, is exactly zero,[1–3] and it has been generally thought that $E_\parallel$ is quite weak and thus its integral along the magnetic field, $F=-\int E_\parallel ds$, is small in low-frequency phenomena in high-temperature plasmas; since $E_\parallel$ contains both longitudinal and transverse components, the quantity F will be referred to as the parallel pseudopotential in this paper. In some particle simulations on electron acceleration in magnetosonic shock waves, however, the observed values of F were quite large.[4] Recently, therefore, the parallel electric field in nonlinear magnetosonic waves has been quantitatively analyzed with theory and electromagnetic particle simulations.[5] The theory and simulations show that F can be large ($E_\parallel$ can be intense), especially when the external magnetic field $\boldsymbol{B}_0$ is strong. The parallel pseudopotential F is given as $eF \sim \epsilon \Gamma_e T_e$ in small-amplitude pulses in a warm plasma with electron temperature T_e, where ϵ is the wave amplitude, and Γ_e is the specific heat ratio of electrons. In a cold plasma such that $\epsilon^2 m_i v_A^2 > \epsilon \Gamma_e T_e$, where v_A is the Alfvén speed, however, it is given as $eF \sim \epsilon^2 m_i v_A^2$. Furthermore, it was found that the simulation results for large-amplitude shock waves with $\epsilon \sim O(1)$ fit fairly well to the phenomenological relation $eF \sim \epsilon(m_i v_A^2+\Gamma_e T_e)$.

The parallel electric field also plays a crucial role in the positron acceleration[6] in oblique shock waves in an electron-positron-ion (e-p-i) plasma (for e-p-i plasmas, see, for instance, Refs. 7–16, and references therein). Indeed, the time rate of change of the Lorentz factor γ of a positron accelerated with this mechanism is proportional to $E_\parallel$, i.e., $\Omega_p^{-1} d\gamma/dt=(c/v_{\rm sh})(\boldsymbol{E}\cdot\boldsymbol{B})/(\boldsymbol{B}\cdot\boldsymbol{B}_0)$, where Ω_p is the positron gyrofrequency, $v_{\rm sh}$ is the shock propagation speed, and $\boldsymbol{B}$ is the total magnetic field at the position of the positron. The Lorentz factors reached ~ 2000 by the end of the simulation run, $\omega_{pe}t=5000$. Furthermore, the simulations revealed an important feature that the positron acceleration becomes weak as the positron density n_{p0} increases. This would also be explained if expressions for $E_\parallel$ and F are known.

It is thus desirable to obtain the parallel electric field in e-p-i plasmas. A theory for nonlinear magnetosonic waves in e-p-i plasmas was developed in Ref. 17, which was, however, based on the cold plasma model ($T=0$) and gave $E_\parallel =0$; the theory therefore cannot be used for the positron acceleration mentioned above. In this paper, extending the work of Ref. 5 to three-component plasmas, we study the parallel electric field $E_\parallel$ and parallel pseudopotential F in nonlinear magnetosonic waves in an e-p-i plasma with theory and simulations.

In Sec. II, we derive the linear dispersion relation of magnetosonic waves propagating obliquely to an external magnetic field in an e-p-i plasma with finite temperatures. The dispersion relation depends on the propagation angle θ as well as the densities and magnetic-field strength, and the dispersion vanishes in the long-wavelength region (the frequency ω is proportional to the wavenumber k) at a critical angle θ_c. This angle decreases from $\theta_c \simeq 88°$ to zero as the positron-to-electron density ratio rises from zero to unity. In Sec. III, we develop a nonlinear theory for small-amplitude waves and obtain $E_\parallel$ and F. It is found that the parallel pseudopotential is proportional to $\epsilon(\Gamma_e p_{e0}-\Gamma_p p_{p0})$ in a warm plasma, where p_{e0} and p_{p0} are, respectively, the electron and positron pressures. For the cold plasma with zero temperatures, we carry out higher order calculations and find that F is proportional to $\epsilon^2 m_i v_A^2/(1+v_A^2/c^2)^3$. In both cases, F decreases with increasing positron density, which accounts for the simulation result[6] that the positron acceleration becomes weak as n_{p0} increases. In a more detailed discussion, we also show the effect of the critical angle θ_c. In Sec. IV, we examine $E_\parallel$ and F by means of one-dimensional, fully kinetic, electromagnetic, particle simulations. First, we test the small-amplitude theory described in Sec. III and find that the simulation results are explained by the theory. Next, we observe F in large-amplitude shock waves with $\epsilon \sim O(1)$ and

[a)]Electronic mail: ohsawa@nagoya-u.jp.

 © 2008 American Institute of Physics

Downloaded 03 Aug 2009 to 133.6.32.19. Redistribution subject to AIP license or copyright; see http://pop.aip.org/pop/copyright.jsp

find that the observed F's are consistent with the phenomenological expression $n_{e0}eF \sim \epsilon(\rho v_A^2 + \Gamma_e p_{e0})(n_{i0}/n_{e0})$, where ρ is the mass density. In Sec. V, we summarize our work. It is mentioned that $E_\parallel$ can be quite strong in high magnetic fields such as those around pulsars.

II. LOW-FREQUENCY, LINEAR MAGNETOSONIC WAVE IN THREE-COMPONENT PLASMA WITH FINITE TEMPERATURES

We obtain here the linear dispersion relation for magnetosonic waves in a three-component plasma consisting of electrons, positrons, and ions with finite temperatures. The set of fluid equations may read as

$$\frac{\partial n_j}{\partial t} + \boldsymbol{\nabla} \cdot (n_j \boldsymbol{v}_j) = 0, \tag{1}$$

$$n_j m_j \left[\frac{\partial}{\partial t} + (\boldsymbol{v}_j \cdot \boldsymbol{\nabla}) \right] \boldsymbol{v}_j = n_j q_j \boldsymbol{E} + \frac{n_j q_j}{c} \boldsymbol{v}_j \times \boldsymbol{B} - \nabla p_j, \tag{2}$$

$$\left[\frac{\partial}{\partial t} + (\boldsymbol{v}_j \cdot \boldsymbol{\nabla}) \right] p_j = -\Gamma_j p_j \nabla \cdot \boldsymbol{v}_j, \tag{3}$$

where the subscript j refers to the electrons ($j=e$), positrons ($j=p$), or ions ($j=i$), and Γ_j denotes the specific heat ratio. These equations are coupled with Maxwell equations. Since the phase velocity of the magnetosonic wave in an e-p-i plasma can be fast, comparable to the speed of light c, the displacement current is included.

By using the mass density,

$$\rho = \sum_j n_{j0} m_j, \tag{4}$$

where the subscript 0 refers to equilibrium quantities, we define the Alfvén speed v_A as

$$v_A = B_0/(4\pi\rho)^{1/2} \tag{5}$$

and $\tilde{v}_A$ as

$$\tilde{v}_A^2 = \frac{v_A^2}{1 + v_A^2/c^2}. \tag{6}$$

Furthermore, we introduce the speeds related to the thermal speeds $v_{Tj} = (T_j/m_j)^{1/2}$,

$$c_j^2 = \Gamma_j v_{Tj}^2 = \Gamma_j \frac{p_{j0}}{n_{j0} m_j}. \tag{7}$$

From the above set of equations, we derive the linear dispersion relation of magnetosonic waves propagating in the x direction in an external magnetic field $\boldsymbol{B}_0 = B_0(\cos\theta, 0, \sin\theta)$. In the limit of $\omega \to 0$, we obtain

$$\frac{c^2}{\tilde{v}_A^2} - \frac{c^2}{v_{mp0}^2} - \frac{\sin^2\theta}{v_{mp0}^2} \sum_j \frac{\omega_{pj}^2 c_j^2/\Omega_j^2}{1 - c_j^2\cos^2\theta/v_{mp0}^2} + \tan^2\theta \left(\sum_j \frac{\omega_{pj}^2/\Omega_j^2}{1 - c_j^2\cos^2\theta/v_{mp0}^2} \right)^2 \Bigg/ \left(\sum_j \frac{\omega_{pj}^2}{1 - c_j^2\cos^2\theta/v_{mp0}^2} \right) = 0, \tag{8}$$

where ω_{pj} is the plasma frequency, Ω_j is the gyrofrequency, and v_{mp0} is the phase velocity ω/k in the low frequency limit (for the details of the calculations, see Appendix A). Assuming that the temperatures are low,

$$\frac{c_j^2}{v_{mp0}^2} \ll 1, \tag{9}$$

we ignore higher order terms of c_j^2/v_{mp0}^2. We then have

$$v_{mp0}^2 = \frac{v_A^2 + c_s^2\sin^2\theta}{1 + v_A^2/c^2}, \tag{10}$$

where c_s is the sound speed,

$$c_s = \left(\frac{n_{i0}\Gamma_i T_{i0} + n_{p0}\Gamma_p T_{p0} + n_{e0}\Gamma_e T_{e0}}{n_{i0}m_i + n_{p0}m_p + n_{e0}m_e} \right)^{1/2}. \tag{11}$$

If we calculate the phase velocity up to the terms of order k^2 (see Appendix B),

$$\frac{\omega}{k} = v_{mp0}(1 + \mu k^2), \tag{12}$$

we find the dispersion coefficient μ as

$$\begin{aligned}\mu = &-\frac{v_{mp0}^2\tilde{v}_A^2}{2c^2}\left[\left(\sum_j \frac{\omega_{pj}^2}{\Omega_j^4} \right) - \frac{\tilde{v}_A^2}{c^2\sin^2\theta} \left(\sum_j \frac{\omega_{pj}^2}{\Omega_j^3} \right)^2 \right] \\ &+ \frac{\tilde{v}_A^2}{c^2}\sin^2\theta \left[\left(\sum_j \frac{\omega_{pj}^2}{\Omega_j^4} c_j^2 \right) - \frac{\tilde{v}_A^2}{c^2\sin^2\theta} \left(\sum_j \frac{\omega_{pj}^2}{\Omega_j^3} \right) \right. \\ &\left. \times \left(\sum_j \frac{\omega_{pj}^2}{\Omega_j^3} c_j^2 \right) \right] + \frac{\tilde{v}_A^2}{c^2\omega_p^2}\cos^2\theta \left(\sum_j \frac{\omega_{pj}^2}{\Omega_j^3} \right) \\ &\times \left(\sum_j \frac{\omega_{pj}^2}{\Omega_j} c_j^2 \right) - \frac{\tilde{v}_A^6 c_s^2}{2c^4 v_A^2 \tan^2\theta} \left(\sum_j \frac{\omega_{pj}^2}{\Omega_j^3} \right)^2. \end{aligned} \tag{13}$$

The sign of μ is important in nonlinear waves. The solitary wave of the magnetosonic wave becomes compressive or rarefactive, according to $\mu < 0$ or $\mu > 0$.[18–20] In the limit of $T_j = 0$, Eq. (13) reduces to

$$\mu = -\frac{\tilde{v}_A^4}{2c^2}\left[\left(\sum_j \frac{\omega_{pj}^2}{\Omega_j^4} \right) - \frac{\tilde{v}_A^2}{c^2\sin^2\theta} \left(\sum_j \frac{\omega_{pj}^2}{\Omega_j^3} \right)^2 \right]. \tag{14}$$

The critical angle θ_c, at which μ becomes zero, is given as

Downloaded 03 Aug 2009 to 133.6.32.19. Redistribution subject to AIP license or copyright; see http://pop.aip.org/pop/copyright.jsp

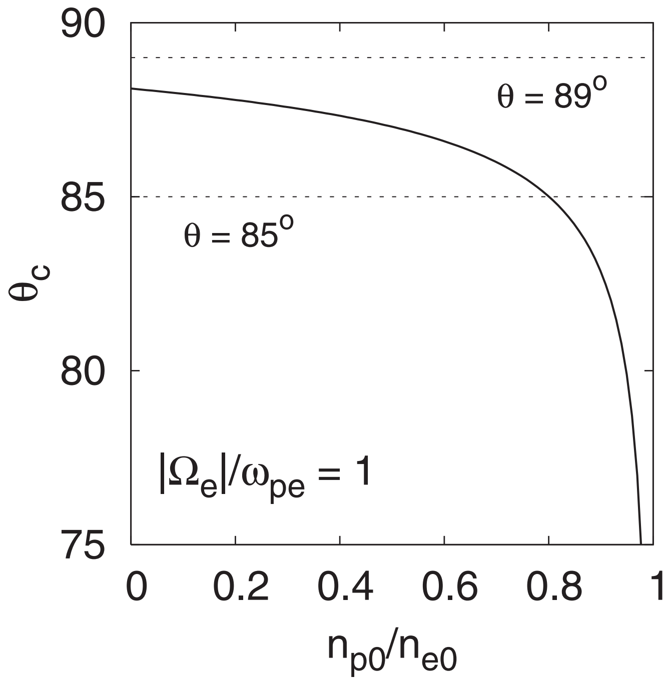

FIG. 1. Critical angle θ_c as a function of n_{p0}/n_{e0}. If the angle θ is 89°, it is always greater than θ_c. If the angle is 85°, it is smaller than θ_c for $n_{p0}/n_{e0} < 0.8007$.

$$\sin\theta_c = \frac{(\tilde{v}_A/c)(\Sigma_j \omega_{pj}^2/\Omega_j^3)}{(\Sigma_j \omega_{pj}^2/\Omega_j^4)^{1/2}} \tag{15}$$

for $T_j = 0$; we see that $\mu > 0$ for $0 < \theta < \theta_c$, and $\mu < 0$ for $\theta_c < \theta < \pi/2$. Figure 1 shows the dependence of the critical angle θ_c given by Eq. (15) on the positron-to-electron density ratio for the case with $m_i/m_e = 1836$, $-q_e = q_p = q_i = e$, and $|\Omega_e|/\omega_{pe} = 1$. As n_{p0}/n_{e0} increases from zero to unity, θ_c goes down from 88.1° to 0°. The decrease is particularly rapid for $n_{p0}/n_{e0} \gtrsim 0.8$. If the propagation angle is $\theta = 89°$, for instance, it is greater than θ_c at all values of n_{p0}/n_{e0}. If $\theta = 85°$, however, it becomes equal to θ_c at $n_{p0}/n_{e0} = 0.8007$.

Outside the vicinities of $n_{p0}/n_{e0} = 1$ and the critical density ratio at which μ becomes zero, $|\mu|$ increases with increasing n_{p0}/n_{e0}. For $v_A^2/c^2 \ll 1$, one finds that

$$\frac{\omega_{pj}^2}{\Omega_j^4} = \frac{4\pi c^4}{e^2 B_0^4} n_{j0} m_j^3, \tag{16}$$

$$\frac{v_A^2}{c^2 \sin^2\theta}\left(\frac{\omega_{pj}^2}{\Omega_j^3}\right)^2 = \frac{4\pi c^4}{e^2 B_0^4 \sin^2\theta}\frac{n_{j0}^2 m_j^4}{\rho}. \tag{17}$$

These relations indicate that the ion terms are dominant in Eq. (14). Moreover their difference,

$$\frac{\omega_{pi}^2}{\Omega_i^4} - \frac{v_A^2}{c^2\sin^2\theta}\frac{\omega_{pi}^4}{\Omega_i^6} \simeq \frac{\omega_{pi}^2}{\Omega_i^4}\left[\left(\frac{n_{e0}+n_{p0}}{n_{i0}}\right)\frac{m_e}{m_i} - \frac{\cos^2\theta}{\sin^2\theta}\right], \tag{18}$$

is also greater than both the electron and positron terms, i.e.,

$$\left|\frac{\omega_{pi}^2}{\Omega_i^4} - \frac{v_A^2}{c^2\sin^2\theta}\frac{\omega_{pi}^4}{\Omega_i^6}\right| \gtrsim \frac{\omega_{pi}^2}{\Omega_i^4}\frac{m_e}{m_i} \gg \frac{\omega_{pe}^2}{\Omega_e^4}, \tag{19}$$

except for the vicinities of $(n_{e0}+n_{p0})/n_{i0} = (m_i/m_e)\cos^2\theta/\sin^2\theta$ and $n_{p0}/n_{e0} = 1$. We thus have

$$\mu \simeq -\frac{v_A^2}{2\Omega_i^2}\frac{n_{i0}m_i}{\rho}\left[\left(\frac{n_{e0}+n_{p0}}{n_{i0}}\right)\frac{m_e}{m_i} - \frac{\cos^2\theta}{\sin^2\theta}\right], \tag{20}$$

which gives

$$\mu \sim -\frac{v_A^2}{2\Omega_i^2}\frac{(n_{e0}+n_{p0})m_e}{\rho} \tag{21}$$

for $\theta > \theta_c$ and

$$\mu \sim \frac{v_A^2}{2\Omega_i^2}\frac{(n_{e0}-n_{p0})m_i}{\rho}\frac{\cos^2\theta}{\sin^2\theta} \tag{22}$$

for $\theta < \theta_c$. Equations (21) and (22) both clearly show that $|\mu|$ increases with increasing n_{p0}/n_{e0}.

III. NONLINEAR MAGNETOSONIC WAVES

Next, we obtain the parallel electric field, $E_\parallel = (\boldsymbol{E}\cdot\boldsymbol{B})/B$, and parallel pseudopotential, $F = -\int E_\parallel ds$, in nonlinear magnetosonic waves. We discuss the finite-temperature case in Sec. III A and zero-temperature case in Sec. III B. In both cases, using the smallness parameter ϵ ($\ll 1$), we introduce stretched coordinates,[21,22]

$$\xi = \epsilon^{1/2}(x - v_{mp0}t), \tag{23}$$

$$\tau = \epsilon^{3/2}t, \tag{24}$$

and expand the plasma variables as[18–20]

$$n_j = n_{j0} + \epsilon n_{j1} + \epsilon^2 n_{j2} + \cdots, \tag{25}$$

$$p_j = p_{j0} + \epsilon p_{j1} + \epsilon^2 p_{j2} + \cdots, \tag{26}$$

$$v_{jx} = \epsilon v_{jx1} + \epsilon^2 v_{jx2} + \cdots, \tag{27}$$

$$v_{jz} = \epsilon v_{jz1} + \epsilon^2 v_{jz2} + \cdots, \tag{28}$$

$$E_y = \epsilon E_{y1} + \epsilon^2 E_{y2} + \cdots, \tag{29}$$

$$B_z = B_0\sin\theta + \epsilon B_{z1} + \epsilon^2 B_{z2} + \cdots, \tag{30}$$

$$v_{jy} = \epsilon^{3/2} v_{jy1} + \epsilon^{5/2} v_{jy2} + \cdots, \tag{31}$$

$$E_x = \epsilon^{3/2} E_{x1} + \epsilon^{5/2} E_{x2} + \cdots, \tag{32}$$

$$E_z = \epsilon^{3/2} E_{z1} + \epsilon^{5/2} E_{z2} + \cdots, \tag{33}$$

$$B_y = \epsilon^{3/2} B_{y1} + \epsilon^{5/2} B_{y2} + \cdots. \tag{34}$$

A. Warm plasma

Applying the above expansion to the three-fluid model and retaining the first order of c_j^2/v_{mp0}^2, we obtain the following Korteweg–de Vries (KdV) equation (for the details, see Appendix C):

$$\frac{\partial B_{z1}}{\partial\tau} + \frac{1}{2}\nu v_{mp0}\frac{B_{z1}}{B_0}\frac{\partial B_{z1}}{\partial\xi} - \mu v_{mp0}\frac{\partial^3 B_{z1}}{\partial\xi^3} = 0, \tag{35}$$

where ν is the nondimensional quantity defined as

Downloaded 03 Aug 2009 to 133.6.32.19. Redistribution subject to AIP license or copyright; see http://pop.aip.org/pop/copyright.jsp

$$\nu = \frac{\tilde{v}_A^2}{v_A^2}\sin\theta\left[3 + \frac{c_s^2}{\tilde{v}_A^2}(-5\sin^2\theta + 3) + \frac{v_A^2\sin^2\theta}{\tilde{v}_A^2 c^2}\left(\sum_j \frac{\omega_{pj}^2}{\Omega_j^2}c_j^2\Gamma_j\right)\right]. \tag{36}$$

In this perturbation scheme, the lowest-order, parallel electric field is given as

$$E_\parallel = \epsilon^{3/2}(E_{x1}\cos\theta + E_{z1}\sin\theta). \tag{37}$$

Substituting Eq. (C28) in Eq. (37) yields

$$E_\parallel = \epsilon^{3/2}\frac{-4\pi e(n_{e0}c_e^2 - n_{p0}c_p^2 - n_{i0}Zc_i^2)}{\omega_p^2}\sin\theta\cos\theta\frac{\partial}{\partial\xi}\left(\frac{B_{z1}}{B_0}\right), \tag{38}$$

where Z is the ionic charge state, $q_i=Ze$, and ω_p^2 is defined as

$$\omega_p^2 = \sum_j \omega_{pj}^2. \tag{39}$$

From Eq. (38), we find the parallel pseudopotential as

$$eF_T = \epsilon\left(\frac{\omega_{pe}^2}{\omega_p^2}\Gamma_e T_e - \frac{\omega_{pp}^2}{\omega_p^2}\Gamma_p T_p - \frac{\omega_{pi}^2}{\omega_p^2}\frac{\Gamma_i T_i}{Z}\right)\sin\theta\frac{B_{z1}}{B_0}. \tag{40}$$

Here, we have used the subscript T to emphasize that F is a function of the temperatures in this case. Since $m_e=m_p \ll m_i$, the contribution of T_i is small; F_T is determined primarily by the difference of the electron and positron pressures. It is noted that as n_{p0}/n_{e0} increases, F_T decreases. A comparison of E_{x1} [Eq. (C30)], E_{z1} [Eq. (C31)], and $E_\parallel$ [Eq. (38)] shows that the terms mainly due to magnetic pressure disappear in $E_\parallel$, i.e., Eq. (C30) and the first term in Eq. (C31) cancel in the sum $E_{x1}\cos\theta + E_{z1}\sin\theta$.

If $n_{p0}/n_{e0}=1$ and $T_p=T_e$, the longitudinal electric field E_x vanishes, i.e., there appears no charge separation.[8] Moreover, as Eqs. (38) and (40) show, $E_\parallel$ and F become zero, although $E_\parallel$ contains the transverse component. In addition, Eqs. (C30), (C31), and (C37) indicate that $E_{x1}=E_{z1}=B_{y1}=0$.

B. Cold plasma

In the limit of $T_j=0$, the parallel electric field Eq. (38) and pseudopotential Eq. (40) vanishes. We now discuss $E_\parallel$ and F in this limit by taking into account higher order terms (for the details of calculation, see Appendix D). We may write the parallel electric field up to the second order terms as

$$E_\parallel = \frac{\boldsymbol{E}\cdot\boldsymbol{B}}{B} = \frac{\boldsymbol{E}_1\cdot\boldsymbol{B}_0}{B_0}\left(1 - \frac{\boldsymbol{B}_1\cdot\boldsymbol{B}_0}{B_0^2}\right) + \frac{\boldsymbol{E}_1\cdot\boldsymbol{B}_1}{B_0} + \frac{\boldsymbol{E}_2\cdot\boldsymbol{B}_0}{B_0}. \tag{41}$$

If $T_j=0$, the lowest order term becomes zero,

$$\frac{\boldsymbol{E}_1\cdot\boldsymbol{B}_0}{B_0} = \epsilon^{3/2}(E_{x1}\cos\theta + E_{z1}\sin\theta) = 0. \tag{42}$$

Furthermore, we see from Eqs. (C7) and (C8) that the term $\boldsymbol{E}_1\cdot\boldsymbol{B}_1$ is zero even when $T_j \neq 0$,

$$\boldsymbol{E}_1\cdot\boldsymbol{B}_1 = \epsilon^{5/2}(E_{y1}B_{y1} + E_{z1}B_{z1}) = 0. \tag{43}$$

We thus have $E_\parallel = \boldsymbol{E}_2\cdot\boldsymbol{B}_0/B_0$. By virtue of Eqs. (D2), (D7), and (D8), we find the parallel electric field in the three-fluid model in the zero temperature limit as

$$E_\parallel = \epsilon^{5/2}(E_{x2}\cos\theta + E_{z2}\sin\theta) = \epsilon^{5/2}\frac{4\pi\tilde{v}_A^4}{B_0^2\tan\theta}\left(\sum_j \frac{n_{j0}m_j^2}{q_j}\right)\left(\frac{c}{\omega_p}\right)^2\frac{\partial^3}{\partial\xi^3}\left(\frac{B_{z1}}{B_0}\right), \tag{44}$$

from which we obtain the parallel pseudopotential as

$$F_B = -\epsilon^2\frac{4\pi\tilde{v}_A^4}{B_0^2\sin\theta}\left(\sum_j \frac{n_{j0}m_j^2}{q_j}\right)\left(\frac{c}{\omega_p}\right)^2\frac{\partial^2}{\partial\xi^2}\left(\frac{B_{z1}}{B_0}\right), \tag{45}$$

for which the magnetic pressure is important; the subscript B is used to show this. In the cold plasma approximation, the parallel pseudopotential is proportional to ϵ^2 and, if $v_A^2 \ll c^2$, proportional to B_0^2, which differs from the finite-temperature case in which F is proportional to ϵ and to temperature. If $n_{i0} \gg (m_e/m_i)n_{e0}$, Eqs. (44) and (45) can be approximated as

$$eE_\parallel = \epsilon^{5/2}\frac{m_i\tilde{v}_A^2}{\tan\theta(1 + v_A^2/c^2)}\left(\frac{c}{\omega_p}\right)^2\frac{\partial^3}{\partial\xi^3}\left(\frac{B_{z1}}{B_0}\right), \tag{46}$$

$$eF_B = -\epsilon^2\frac{m_i\tilde{v}_A^2}{\sin\theta(1 + v_A^2/c^2)}\left(\frac{c}{\omega_p}\right)^2\frac{\partial^2}{\partial\xi^2}\left(\frac{B_{z1}}{B_0}\right). \tag{47}$$

In the limit of $n_{p0}=0$ ($\omega_p \simeq \omega_{pe}$), Eq. (47) reduces to F in the two-fluid model in the cold plasma limit.[5]

At $n_{p0}/n_{e0}=1$, both $E_\parallel$ and F are zero, which we see from Eqs. (44) and (45). Thus, the relation $E_\parallel=0$ holds for both warm and cold plasmas if $n_{p0}/n_{e0}=1$.

For a stationary solitary pulse with a magnetic-field amplitude $B_{z1}=B_{z1\text{peak}}$, the peak value of F is given as

$$eF_{\text{peak}} = -\frac{m_i\tilde{v}_A^2}{4}\left[\frac{(n_{e0}-n_{p0})m_i}{\rho}\right] \times\left(\frac{1}{Z^2} - \frac{m_e^2}{m_i^2}\right)\frac{(c/\omega_p)^2}{\mu}\left(\frac{\tilde{v}_A}{v_A}\right)^4\left(\frac{B_{z1\ \text{peak}}}{B_0}\epsilon\right)^2. \tag{48}$$

Figures 2 and 3 show the dependence of F_{peak} on the positron density; here, we have normalized F to the value of F at $n_{p0}=0$. In Fig. 2, the propagation angle is $\theta=89°$ and is greater than θ_c for all values of n_{p0}/n_{e0}. The value of F_{peak} monotonically decreases as n_{p0}/n_{e0} varies from zero to unity. In Fig. 3, θ is 85° and becomes equal to θ_c at $n_{p0}/n_{e0}=0.8007$; F_{peak} diverges at this density ratio. Outside this small region, however, F_{peak} decreases with increasing n_{p0}/n_{e0}. In fact, by substituting μ given by Eqs. (21) and (22) in Eq. (48), we can express the dependence of F on n_{p0}/n_{e0} for the case $v_A^2 \ll c^2$ as

$$F \propto \frac{1 - n_{p0}/n_{e0}}{(1 + n_{p0}/n_{e0})[1 + n_{p0}/n_{e0} + (1 - n_{p0}/n_{e0})m_e/m_i]} \tag{49}$$

for $\theta > \theta_c$ and

Downloaded 03 Aug 2009 to 133.6.32.19. Redistribution subject to AIP license or copyright; see http://pop.aip.org/pop/copyright.jsp

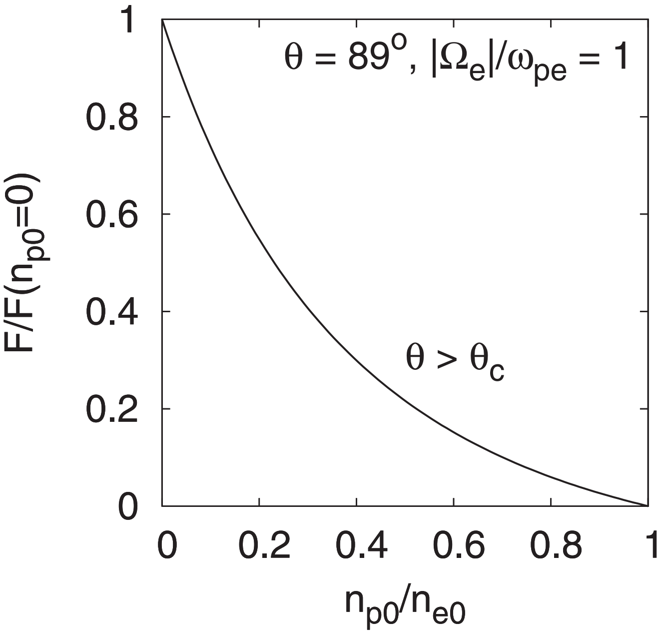

FIG. 2. Peak value of F of the solitary wave as a function of n_{p0}/n_{e0}. Here, θ is 89° and is greater than θ_c.

$$F \propto \frac{1}{1+n_{p0}/n_{e0}+(1-n_{p0}/n_{e0})m_e/m_i} \tag{50}$$

for $\theta<\theta_c$. These indicate that except for the vicinity of the critical density ratio, F decreases with increasing n_{p0}/n_{e0}.

The behavior of the electric potential ϕ is quite different from that of F. We have an analytic expression for ϕ as

$$\phi = \frac{\tilde{v}_A^4 B_0}{c^3 \sin\theta}\sum_j \frac{\omega_{pj}^2}{\Omega_j^3}\left(\frac{B_{z1}}{B_0}\epsilon\right), \tag{51}$$

from which we see its density dependence as

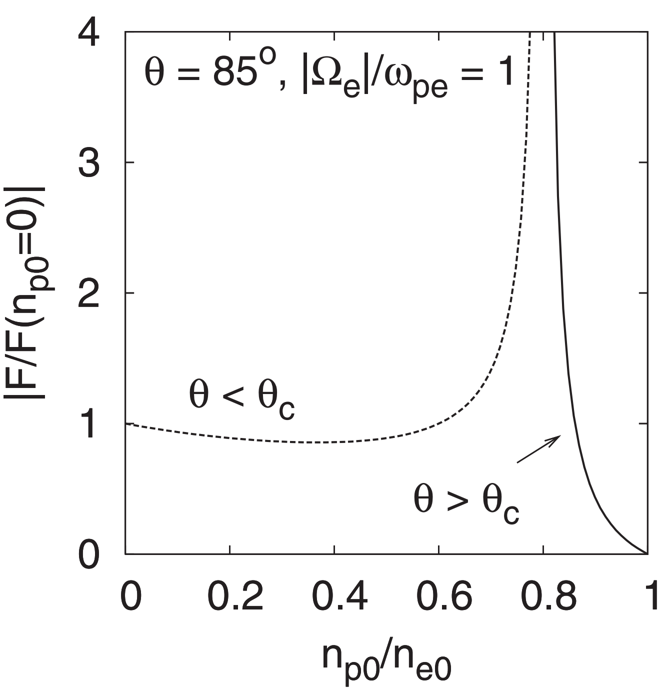

FIG. 3. Peak value of F of the solitary wave. Here, θ is 85° and is smaller than θ_c for $n_{p0}/n_{e0}<0.8007$, for which F is negative.

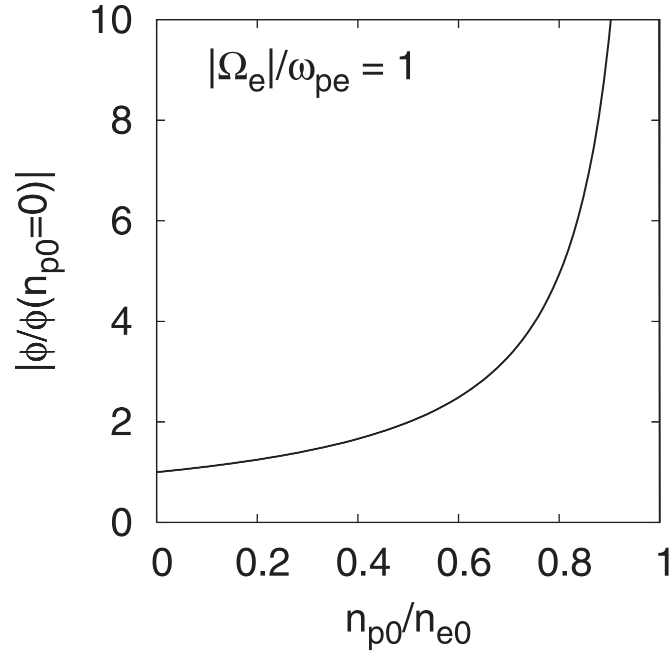

FIG. 4. Electric potential ϕ vs n_{p0}/n_{e0}. Although θ is 85°, there is no singularity.

$$|\phi| \propto \tilde{v}_A^4(n_{e0}-n_{p0}). \tag{52}$$

As n_{p0}/n_{e0} rises, $\tilde{v}_A$ and thus $|\phi|$ increase. The electric potential does not diverge at any value of n_{p0}/n_{e0}. Figure 4 shows the electric potential ϕ as a function of n_{p0}/n_{e0}; the parameters are the same as those in Fig. 3. For most of the region, $0<n_{p0}/n_{e0}\lesssim 0.998$, ϕ increases with n_{p0}/n_{e0}. As shown in Fig. 5, it rapidly goes down to zero in a very narrow region, $0.998\lesssim n_{p0}/n_{e0}\leqslant 1$.

In the simulations in the next section, F is mainly discussed, because $E_\parallel$ is easily masked by thermal noise and is more difficult to measure. With the help of the relation

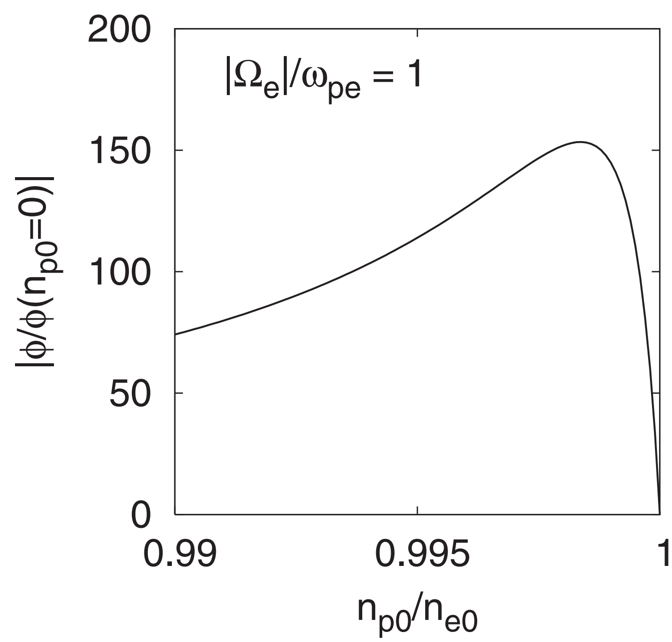

FIG. 5. Electric potential ϕ near $n_{p0}/n_{e0}=1$.

Downloaded 03 Aug 2009 to 133.6.32.19. Redistribution subject to AIP license or copyright; see http://pop.aip.org/pop/copyright.jsp

$$F = -\int E_{\parallel} ds = -\int E_{\parallel} \frac{B}{B_{x0}} dx, \tag{53}$$

we can make an order estimation of $E_{\parallel}$ by using F,

$$\langle E_{\parallel} \rangle \sim \frac{B_{x0}}{\langle B \rangle} \frac{F}{\Delta}, \tag{54}$$

where Δ is the width of a shock transition region (or the width of a soliton) and the brackets indicate the average over this region. Equation (54) is consistent with the relation between $E_{\parallel}$ and F in warm plasmas [Eqs. (38) and (40)] and with that in cold plasmas [Eqs. (44) and (45)]. Similarly, we have $\langle E_x \rangle \sim \phi/\Delta$ and find that

$$\frac{\langle E_{\parallel} \rangle}{\langle E_x \rangle} \sim \frac{B_{x0}}{\langle B \rangle} \frac{F}{\phi}. \tag{55}$$

IV. SIMULATION OF WAVE EVOLUTION AND PARTICLE ACCELERATION

We now study the parallel electric field by means of one-dimensional, fully kinetic, electromagnetic, particle simulations,[23] in which we generate magnetosonic pulses and observe their propagation. We take the mass ratios to be $m_i/m_e=400$ and $m_p/m_e=1$, with their charges $q_i=q_p=-q_e$. The speed of light is $c/(\omega_{pe}\Delta_g)=10$, where Δ_g is the grid spacing, and the ion thermal velocity is fixed to be $(T_i/m_i)^{1/2}/(\omega_{pe}\Delta_g)=0.013$. We test high ($F_T \gg F_B$) and low ($F_B \gg F_T$) beta cases (beta is the ratio of thermal to magnetic pressures); in the former, the magnetic-field strength and electron thermal velocity are, respectively, $|\Omega_e|/\omega_{pe}=0.5$ and $v_{Te}/(\omega_{pe}\Delta_g)=2.0$ ($T_e=60T_i$), and in the latter, $|\Omega_e|/\omega_{pe}=1.0$ and $v_{Te}/(\omega_{pe}\Delta_g)=0.26$ ($T_e=T_i$). In both cases, T_p is equal to T_e.

We discuss small-amplitude pulses and shock waves separately below. In the former, the system length is $L=2048\Delta_g$ with the total number of electrons $N_e \simeq 4.9\times 10^6$, while in the latter, $L=16384\Delta_g$ with $N_e \simeq 6.1\times 10^5$. (We use a greater number of simulation particles for the small-amplitude case to reduce noise.[24])

A. Small-amplitude pulses

First, we examine small-amplitude pulses and compare them with the nonlinear theory in Sec. III. Figure 6 shows the magnitude of F in a small-amplitude pulse with $\theta=88°$ as a function of n_{p0}/n_{e0} for the case $F_T \gg F_B$. Both the theory (40) (solid line) and simulation results (dots) decrease with increasing n_{p0}/n_{e0}. Here, since the theory (40) for F_T predicts that F is proportional to the amplitude ϵ (and thus F/ϵ should be independent of ϵ), we have plotted the values of F/ϵ; and they are normalized to the value of F/ϵ at $n_{p0}/n_{e0}=0$. The pulse amplitudes used in Fig. 6 were in the range $0.075 < B_{z1}/B_0 < 0.085$.

The method of measurement of F, which is small and can be masked by thermal noise, is described in Ref. 5. We make use of the fact that other quantities such as B_z are much easier to measure. From the profiles of $B_z(x,t_j)$ in a pulse at consecutive times t_j ($j=1,2,\ldots,N$), we obtain the pulse speed $v_{\rm sh}$. We then average the profiles of $F(x-v_{\rm sh}t_j, t_j)$ over time, which smooths out the fluctuations.

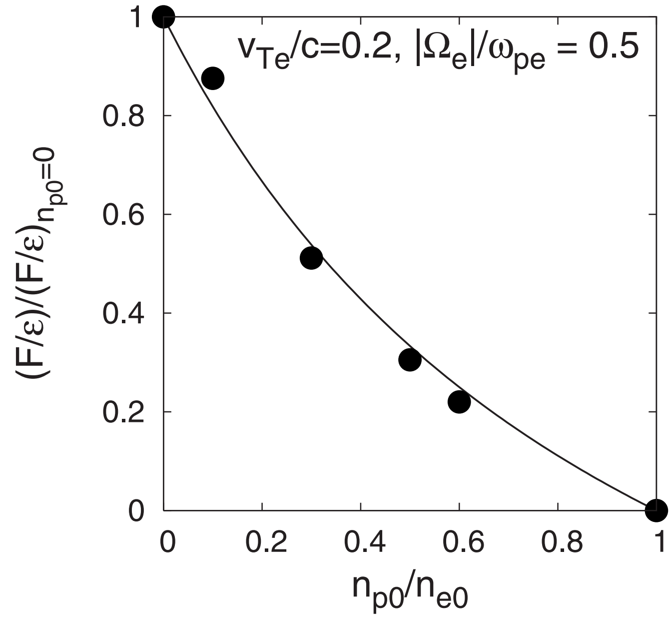

FIG. 6. Magnitude of F/ϵ of small-amplitude pulse as a function of n_{p0}/n_{e0} for the case $F_T \gg F_B$. Here, $(F/\epsilon)_{n_{p0}=0}$ denotes the value of F/ϵ at $n_{p0}/n_{e0}=0$.

Figures 7 and 8 show the dependence of F on the positron density for the case $F_B \gg F_T$, for which F given by Eq. (48) is proportional to ϵ^2; therefore F/ϵ^2 is plotted. In Fig. 7, the propagation angle ($\theta=88°$) is greater than θ_c for all values of n_{p0}/n_{e0}, and thus F monotonically decreases as n_{p0}/n_{e0} rises from zero to unity. In Fig. 8, on the other hand, the propagation angle ($\theta=85°$) becomes equal to θ_c at $n_{p0}/n_{e0}=0.26$, around which F becomes quite large. Outside the vicinity of this point, F decreases with increasing positron density. The amplitudes in Fig. 7 were in the range $0.095 < B_{z1}/B_0 < 0.10$, and those in Fig. 8 were in $0.0087 < |B_{z1}/B_0| < 0.099$.

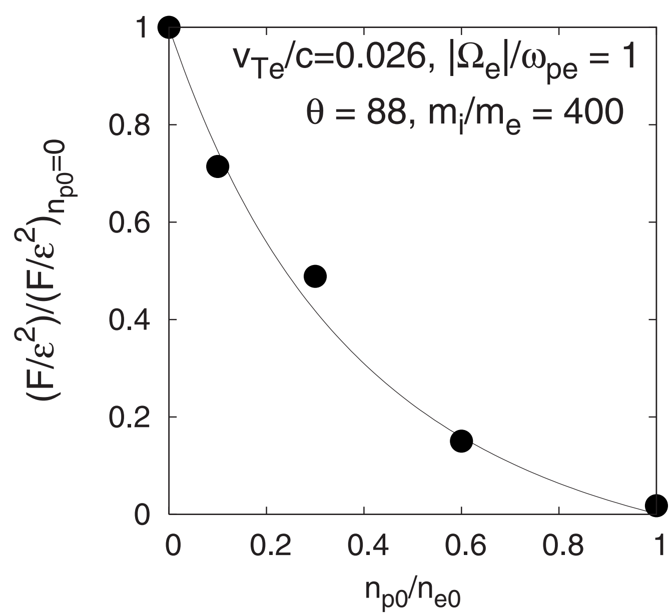

FIG. 7. Dependence of F/ϵ^2 on n_{p0}/n_{e0} for the case $F_B \gg F_T$. Here, the propagation angle is 88° and is greater than θ_c.

Downloaded 03 Aug 2009 to 133.6.32.19. Redistribution subject to AIP license or copyright; see http://pop.aip.org/pop/copyright.jsp

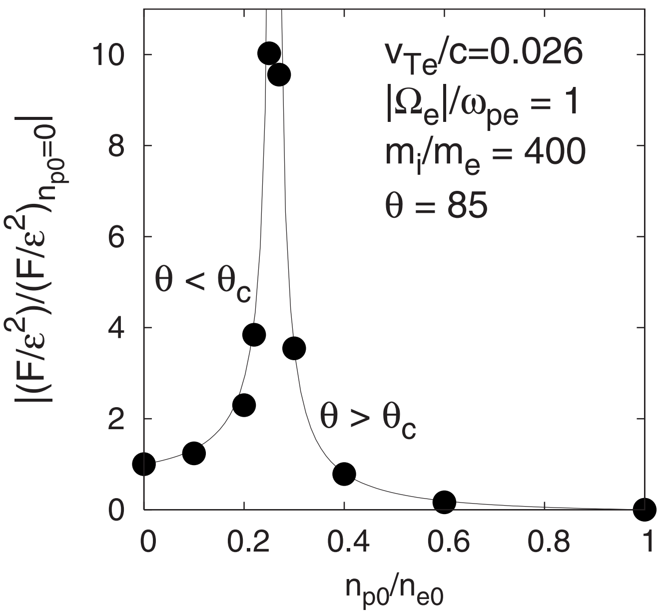

FIG. 8. Dependence of F/ϵ^2 on n_{p0}/n_{e0} for the case $F_B \gg F_T$. Here, the propagation angle is 85° and becomes equal to θ_c at $n_{p0}/n_{e0}=0.26$.

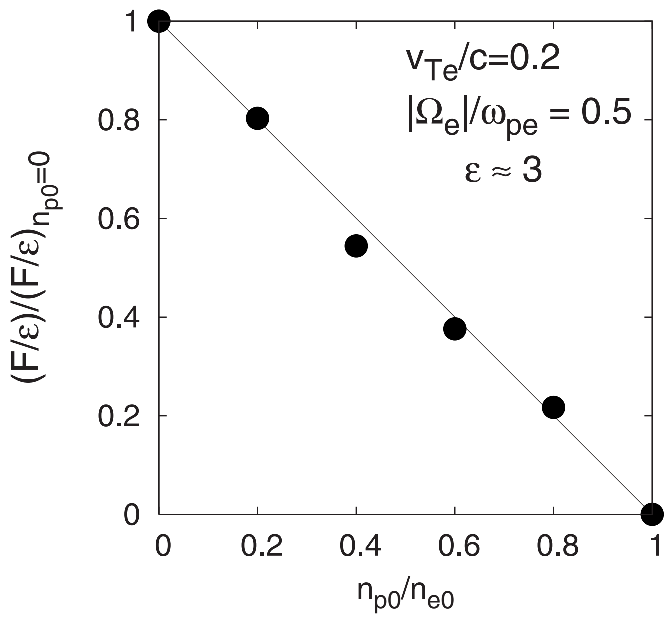

FIG. 10. Parallel pseudopotential F in the shock wave for the higher beta case. The propagation angle is $\theta=60°$.

The dependence of the electric potential ϕ on n_{p0} is quite different from that of F, as shown in Fig. 9, where the dots and white triangles show, respectively, the simulation values for $\theta=88°$ and $\theta=85°$ (other simulation parameters are the same as those in Figs. 7 and 8). The value of ϕ increases with increasing positron density, except near the point $n_{p0}/n_{e0}=1$, at which ϕ becomes zero. In Figs. 7–9, the theory and simulation results are consistent.

B. Shock waves

The theory in Sec. III and simulations in Sec. IV A were concerned with small-amplitude waves with $\epsilon \ll 1$. Here, we examine large-amplitude waves (shock waves) with $\epsilon \sim O(1)$ with simulations. Figures 10 and 11 show F/ϵ in shock waves with $2 \lesssim \epsilon \lesssim 5$ and $\theta=60°$ as a function of the positron density. Although the plasma beta value in Fig. 10 and that in Fig. 11 are quite different, the simulation results fit fairly well to a phenomenological relation (solid line) in both cases. This relation is

$$eF \sim \left(\frac{B_0^2}{4\pi n_{e0}} + \Gamma_e T_e\right)\left(1 - \frac{n_{p0}}{n_{e0}}\right)\frac{B_{z1}}{B_0}, \tag{56}$$

for which a rigorous mathematical theory has not been given yet. These results indicate that in large-amplitude waves, the term related to B_0^2 and that to T_e are both proportional to the

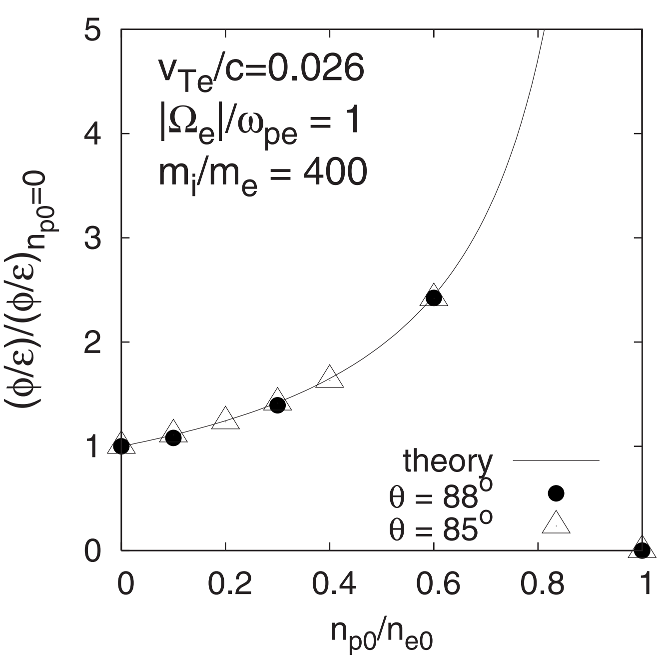

FIG. 9. Electric potential ϕ/ϵ vs positron density. The dots and triangles show, respectively, the simulation values for $\theta=88°$ and $\theta=85°$.

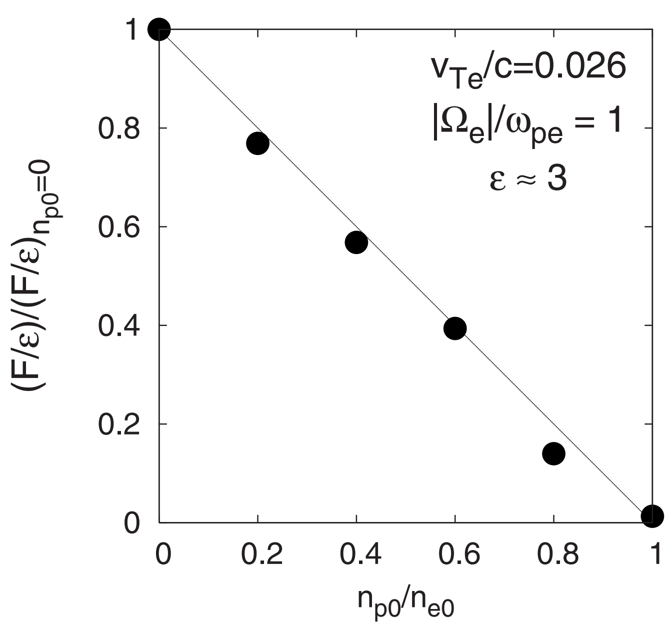

FIG. 11. Parallel pseudopotential F in the shock wave for the lower beta case.

Downloaded 03 Aug 2009 to 133.6.32.19. Redistribution subject to AIP license or copyright; see http://pop.aip.org/pop/copyright.jsp

amplitude ϵ $(=B_{z1}/B_0)$, as in the case of two-component plasmas.[5]

We make a short mention of the measurement of F again. The profiles of B_z and F are not perfectly stationary; they tend to alternately have steep and diffusive profiles in the transition region.[25] For the data points for $0 \leqslant n_{p0}/n_{e0} \leqslant 0.6$, we have plotted the values of F averaged over a period $\omega_{pe}t \simeq 200$ for which the B_z profile was steep. At $n_{p0}/n_{e0}=0.8$, however, since the nonstationarity of F is more enhanced, we have taken an average for a much longer time, $\omega_{pe}t \simeq 2000$. Shock profiles become more unstable as n_{p0}/n_{e0} increases. (At $n_{p0}/n_{e0}=1$, however, F is always close to zero.) The time-dependence of shock profiles in e-p-i plasmas will be discussed elsewhere.

We may write Eq. (56) in terms of energy density as

$$n_{e0}eF \sim (\rho v_A^2 + \Gamma_e p_{e0}) \frac{n_{i0}}{n_{e0}} \frac{B_{z1}}{B_0}. \tag{57}$$

We note that the parallel pseudopotential obtained for a shock wave in a two-component plasma,[5]

$$eF \sim (m_i v_A^2 + \Gamma_e T_e) \frac{B_{z1}}{B_0}, \tag{58}$$

can also be put into this form. That is, if we express F in the form of Eq. (57), it is applicable to both two- and three-component plasmas.

V. SUMMARY

We have studied the parallel electric field in nonlinear magnetosonic waves in e-p-i plasmas with theory and fully kinetic, electromagnetic, particle simulations. The theory based on the three-fluid model predicts that the parallel pseudopotential F $(=-\int E_\parallel ds)$ in small-amplitude waves with $\epsilon \ll 1$ is proportional to $\epsilon(\Gamma_e p_{e0} - \Gamma_p p_{p0})$ in warm plasmas and to $\epsilon^2 m_i v_A^2/(1+v_A^2/c^2)^3$ in cold plasmas. The dispersion coefficient μ becomes zero at propagation angle θ_c, which varies with n_{p0}/n_{e0}. The effect of such angle has also been discussed. The magnitude of F decreases as n_{p0}/n_{e0} increases, except for the vicinity of the point at which μ becomes zero. We then examined the parallel electric field with electromagnetic particle simulations, the result of which was explained by the present theory. Furthermore, for shock waves with $\epsilon \sim O(1)$, the simulation values are found to be consistent with the phenomenological relation $n_{e0}eF \sim \epsilon(\rho v_A^2 + \Gamma_e p_{e0}) \times (n_{i0}/n_{e0})$.

These results indicate that $E_\parallel$ can be strong in plasmas in high magnetic fields. This implies that extremely strong parallel electric fields can be generated around pulsars,[7] which rotate rapidly with very strong magnetic fields and can have e-p-i plasmas around them.

In addition, the expression for F in a shock wave, Eq. (57), indicates that some positrons can be reflected by the shock wave along the magnetic field when the magnetic field is weak as well as when it is strong. We see this because in the wave frame the flow speed of upstream positrons is $\sim v_A$ for a low beta case and is $\sim (T_e/m_i)^{1/2}$ for a high beta case and therefore the kinetic energy of the positrons entering the shock wave can be smaller than eF unless n_{i0} is very close to zero. Thus, even in high beta (weak magnetic field) cases, the parallel electric field can greatly affect the motions of positrons.

In the future, it would be desirable to obtain the phenomenological relation (57) with a rigorous theory. Furthermore, it will be interesting and important to develop a relativistic theory on the parallel electric field in extremely strong magnetic fields.[26]

ACKNOWLEDGMENTS

This work was carried out by the joint research program of the Solar-Terrestrial Environment Laboratory, Nagoya University, and by the collaboration program, NIFS06KTAT017, of the National Institute for Fusion Science.

APPENDIX A: LINEAR DISPERSION RELATION

We derive here the linear dispersion relation of the magnetosonic wave with a wavenumber $\boldsymbol{k}=(k,0,0)$ in an e-p-i plasma in an external magnetic field $\boldsymbol{B}_0 = B_0(\cos\theta, 0, \sin\theta)$.

We expand the variables as, for instance,

$$\boldsymbol{B} = \boldsymbol{B}_0 + \boldsymbol{B}_1 \exp[i(kx - \omega t)], \tag{A1}$$

and linearize the set of fluid equations. Then, after some algebra, we find the following relation:

$$\begin{aligned}
&\left[1 - \sum_j \frac{\omega_{pj}^2}{R_j} - \frac{k^2}{\omega^2}\left(c^2 - \sum_j \frac{\omega_{pj}^2 c_j^2}{R_j}\right)\right] \times \left\{\left[1 - \sum_j \frac{\omega_{pj}^2(\omega^2 - \Omega_j^2)}{R_j \omega^2}\right]\left[1 - \sum_j \frac{\omega_{pj}^2}{R_j} - \frac{k^2}{\omega^2}\left(c^2 - \sum_j \frac{\omega_{pj}^2 c_j^2}{R_j}\right)\right]\right. \\
&\quad \left. + \frac{1}{\omega^2}\left(\sum_j \frac{\omega_{pj}^2 \Omega_j^2}{R_j}\right)\frac{k^2}{\omega^2}\left(c^2 - \sum_j \frac{\omega_{pj}^2 c_j^2}{R_j}\right)\sin^2\theta\right\} - \frac{\sin^2\theta}{\omega^2}\left(\sum_j \frac{\omega_{pj}^2 \Omega_j}{R_j}\right)^2 \left[1 - \sum_j \frac{\omega_{pj}^2}{R_j} - \frac{k^2}{\omega^2}\left(c^2 - \sum_j \frac{\omega_{pj}^2 c_j^2}{R_j}\right)\right] \\
&\quad - \frac{1}{\omega^4}\left(\sum_j \frac{\omega_{pj}^2 \Omega_j^2}{R_j}\right)\left[\left(\sum_j \frac{\omega_{pj}^2 \Omega_j}{R_j}\right) - \left(\sum_j \frac{\omega_{pj}^2 \Omega_j c_j^2}{R_j}\right)\frac{k^2}{\omega^2}\cos^2\theta\right]^2 - \frac{\cos^2\theta}{\omega^2}\left(1 - \sum_j \frac{\omega_{pj}^2}{R_j}\right)\left[\left(\sum_j \frac{\omega_{pj}^2 \Omega_j}{R_j}\right)\right. \\
&\quad \left. - \left(\sum_j \frac{\omega_{pj}^2 \Omega_j c_j^2}{R_j}\right)\frac{k^2}{\omega^2}\right]^2 = 0,
\end{aligned} \tag{A2}$$

Downloaded 03 Aug 2009 to 133.6.32.19. Redistribution subject to AIP license or copyright; see http://pop.aip.org/pop/copyright.jsp

where

$$R_j = \omega^2 - \Omega_j^2 - c_j^2 k^2\left(1 - \frac{\Omega_j^2}{\omega^2}\cos^2\theta\right). \tag{A3}$$

Equation (A2) includes dispersion relations of several different plasma waves. We now consider low-frequency waves with $\omega^2 \ll \Omega_i^2$ and approximate $1/R_j$ as

$$\frac{1}{R_j} \simeq -\frac{1}{\Omega_j^2(1 - c_j^2 k^2\cos^2\theta/\omega^2)}. \tag{A4}$$

With use of the relations

$$\sum_j \frac{\omega_{pj}^2/\Omega_j}{1 - c_j^2 k^2 \cos^2\theta/\omega^2} = \frac{k^2}{\omega^2}\cos^2\theta \sum_j \frac{\omega_{pj}^2 c_j^2/\Omega_j}{1 - c_j^2 k^2\cos^2\theta/\omega^2}, \tag{A5}$$

$$\sum_j \frac{\omega_{pj}^2/\Omega_j^2}{1 - c_j^2 k^2\cos^2\theta/\omega^2} = \sum_j \frac{\omega_{pj}^2}{\Omega_j^2} + \frac{k^2}{\omega^2}\cos^2\theta \times \sum_j \frac{\omega_{pj}^2 c_j^2/\Omega_j^2}{1 - c_j^2 k^2 \cos^2\theta/\omega^2}, \tag{A6}$$

$$\sum_j \frac{\omega_{pj}^2}{\Omega_j^2} = \frac{c^2}{v_A^2}, \tag{A7}$$

$$1 + \sum_j \frac{\omega_{pj}^2}{\Omega_j^2} = \frac{c^2}{\tilde{v}_A^2}, \tag{A8}$$

Eq. (A2) reduces, in the limit of $\omega \to 0$, to

$$\left(\frac{1}{\tilde{v}_A^2} - \frac{\cos^2\theta}{v_{p0}^2}\right)\left[\frac{c^2}{\tilde{v}_A^2} - \frac{c^2}{v_{p0}^2} - \frac{\sin^2\theta}{v_{p0}^2}\sum_j \frac{\omega_{pj}^2 c_j^2/\Omega_j^2}{1 - c_j^2\cos^2\theta/v_{p0}^2} + \tan^2\theta\left(\sum_j \frac{\omega_{pj}^2/\Omega_j}{1 - c_j^2\cos^2\theta/v_{p0}^2}\right)^2 \Bigg/ \left(\sum_j \frac{\omega_{pj}^2}{1 - c_j^2\cos^2\theta/v_{p0}^2}\right)\right] = 0, \tag{A9}$$

where v_{p0} is the phase velocity ω/k in the low frequency limit. The first parentheses give the shear Alfvén wave, $v_{Ap0} = \tilde{v}_A\cos\theta$, and the square brackets give the magnetosonic wave (8). If the thermal speeds are low, $c_j^2/v_{mp0}^2 \ll 1$, using the relation

$$\sum_j \frac{\omega_{pj}^2 c_j^2}{\Omega_j^2} = \frac{c^2 c_s^2}{v_A^2} \tag{A10}$$

we obtain Eq. (10) from Eq. (8).

APPENDIX B: LINEAR DISPERSION RELATION FOR SMALL BUT FINITE WAVENUMBERS

The magnetosonic wave has weak dispersion of the form (12). We here calculate the dispersion coefficient μ.

We define the quantities α_j and β_j as

$$\alpha_j = \frac{1}{(1 - c_j^2 k^2\cos^2\theta/\omega^2)}, \tag{B1}$$

$$\beta_j = \frac{(1 - c_j^2 k^2/\omega^2)}{(1 - c_j^2 k^2\cos^2\theta/\omega^2)^2}. \tag{B2}$$

Then, since $\omega^2/\Omega_i^2 \ll 1$, we can write $1/R_j$ as

$$\frac{1}{R_j} \simeq -\frac{1}{\Omega_j^2}\left(\alpha_j + \beta_j \frac{\omega^2}{\Omega_j^2}\right). \tag{B3}$$

We substitute Eq. (B3) in Eq. (A2) and retain the terms up to ω^2/Ω_j^2. Then, by virtue of the assumption that $v_p^2 \gg c_j^2$, where $v_p = \omega/k$, we find that

$$\begin{aligned}
&\left[\sum_j \omega_{pj}^2\left(1 + \frac{c_j^2}{v_p^2}\cos^2\theta\right)\right]\left(\frac{c^2}{\tilde{v}_A^2} - \frac{c^2}{v_p^2}\cos^2\theta\right)\left(\frac{c^2}{\tilde{v}_A^2} - \frac{c^2}{v_p^2} - \frac{c^2 c_s^2}{v_p^2 v_A^2}\sin^2\theta\right) + \left[\sum_j \omega_{pj}^2\left(1 + \frac{c_j^2}{v_p^2}\cos^2\theta\right)\right]\Bigg\{\left(\frac{c^2}{\tilde{v}_A^2} - \frac{c^2}{v_p^2}\cos^2\theta\right) \\
&\times\left[\sum_j \frac{\omega_{pj}^2}{\Omega_j^4}\left(1 - 2\frac{c_j^2}{v_p^2}\sin^2\theta\right)\right] + \left(\frac{c^2}{\tilde{v}_A^2} - \frac{c^2}{v_p^2} - \frac{c^2 c_s^2}{v_p^2 v_A^2}\sin^2\theta\right)\left[\sum_j \frac{\omega_{pj}^2}{\Omega_j^4}\left(1 - \frac{c_j^2}{v_p^2}\sin^2\theta\right)\right] - \left[\sum_j \frac{\omega_{pj}^2}{\Omega_j^3}\left(1 - \frac{c_j^2}{v_p^2}\sin^2\theta\right)\right]^2\Bigg\}\omega^2 \\
&-\left(\frac{c^2}{\tilde{v}_A^2} - \frac{c^2}{v_p^2} - \frac{c^2 c_s^2}{v_p^2 v_A^2}\sin^2\theta\right)\left[\left(\frac{c^2}{\tilde{v}_A^2} + \frac{c^2 c_s^2}{v_p^2 v_A^2}\cos^2\theta\right)\left(\frac{c^2}{\tilde{v}_A^2} - \frac{c^2}{v_p^2} - \frac{c^2 c_s^2}{v_p^2 v_A^2}\sin^2\theta\right) - \left(\frac{c^2}{\tilde{v}_A^2} - \frac{c^2}{v_p^2}\cos^2\theta\right)\right. \\
&\left.\times\left(\frac{c^2}{v_A^2} + \frac{c^2 c_s^2}{v_p^2 v_A^2}\cos 2\theta\right)\right]\omega^2 - 2\frac{\sin^2\theta\cos^2\theta}{v_p^2}\left(\sum_j \frac{\omega_{pj}^2 c_j^2}{\Omega_j}\right)\Bigg\{\left(\frac{c^2}{\tilde{v}_A^2} + \frac{c^2 c_s^2}{v_p^2 v_A^2}\cos^2\theta\right)\left[\sum_j \frac{\omega_{pj}^2}{\Omega_j^3}\left(1 - 2\frac{c_j^2}{v_p^2}\sin^2\theta\right)\right] \\
&-\left[\sum_j \frac{\omega_{pj}^2}{\Omega_j^3}\left(1 + \frac{c_j^2}{v_p^2}\cos 2\theta\right)\right]\left(\frac{c^2}{\tilde{v}_A^2} - \frac{c^2}{v_p^2} - \frac{c^2 c_s^2}{v_p^2 v_A^2}\sin^2\theta\right)\Bigg\}\omega^2 = 0.
\end{aligned} \tag{B4}$$

Downloaded 03 Aug 2009 to 133.6.32.19. Redistribution subject to AIP license or copyright; see http://pop.aip.org/pop/copyright.jsp

For small but finite wavenumbers, we write the phase velocity as

$$v_p(k) \simeq v_{mp0} + \delta v_p(k), \tag{B5}$$

where $\delta v_p(k)$ is much smaller than v_{mp0}. We multiply Eq. (B4) by $v_p^6 \tilde{v}_A^4/c^4$ and substitute Eq. (B5) for v_p. Then, calculating up to the terms of order k^2, and using the relation (10), we find that $\delta v_p(k) = v_{mp0}\mu k^2$, where μ is the dispersion coefficient given by Eq. (13).

APPENDIX C: DERIVATION OF THE KDV EQUATION

We derive the KdV equation for magnetosonic waves in an e-p-i plasma with finite temperatures.

1. Perturbations

We apply the stretching and expansion (23)–(34) to the set of basic fluid equations. Then, for instance, from the continuity equation, we have

$$\epsilon^{3/2}\frac{\partial}{\partial \xi}(n_{j0}v_{jx1} - v_{mp0}n_{j1}) + \epsilon^{5/2}\left[\frac{\partial n_{j1}}{\partial \tau} - v_{mp0}\frac{\partial n_{j2}}{\partial \xi} + n_{j0}\frac{\partial v_{jx2}}{\partial \xi} + \frac{\partial (n_{j1}v_{jx1})}{\partial \xi}\right] + \cdots = 0. \tag{C1}$$

Similarly, from Eqs. (2) and (3) and Maxwell equations, we have equations for perturbed quantities. From the lowest order equations, we obtain the following relations among the lowest order quantities:

$$n_{j1} = \frac{n_{j0}}{v_{mp0}}v_{jx1}, \tag{C2}$$

$$v_{jy1} = -\frac{cE_{x1}}{B_0 \sin\theta} + \frac{v_{mp0}}{\Omega_j \sin\theta}\left(\frac{\Gamma_j p_{j0}}{m_j n_{j0}}\frac{1}{v_{mp0}^2} - 1\right)\frac{\partial v_{jx1}}{\partial \xi}, \tag{C3}$$

$$v_{jz1} = v_{jx1}\tan\theta - \frac{v_{mp0}B_{z1}}{B_0\cos\theta}, \tag{C4}$$

$$v_{jy1} = \frac{cE_{z1}}{B_0\cos\theta} + \frac{v_{mp0}}{\Omega_j\cos\theta}\frac{\partial v_{jz1}}{\partial \xi}, \tag{C5}$$

$$p_{j1} = \frac{\Gamma_j p_{j0}}{v_{mp0}}v_{jx1}, \tag{C6}$$

$$E_{z1} = -\frac{v_{mp0}}{c}B_{y1}, \tag{C7}$$

$$E_{y1} = \frac{v_{mp0}}{c}B_{z1}, \tag{C8}$$

$$\sum_j n_{j0}q_j v_{jx1} = 0, \tag{C9}$$

$$\sum_j n_{j0}q_j v_{jy1} = -\left(1 - \frac{v_{mp0}^2}{c^2}\right)\frac{\partial B_{z1}}{\partial \xi}, \tag{C10}$$

$$\sum_j n_{j0}q_j v_{jz1} = 0. \tag{C11}$$

2. Higher order quantities

The relations among the second lowest order terms ($\sim\epsilon^2$ or $\epsilon^{5/2}j$) may be written as

$$\frac{\partial n_{j1}}{\partial \tau} + \frac{\partial}{\partial \xi}(n_{j1}v_{jx1}) - v_{mp0}\frac{\partial n_{j2}}{\partial \xi} + n_{j0}\frac{\partial v_{jx2}}{\partial \xi} = 0, \tag{C12}$$

$$\begin{aligned}&\frac{\partial v_{jx1}}{\partial \tau} + \left(1 - \frac{\Gamma_j p_{j0}}{m_j n_{j0}}\frac{1}{v_{mp0}^2}\right)v_{jx1}\frac{\partial v_{jx1}}{\partial \xi} \\ &+ \Omega_j\frac{B_{y1}}{B_0}\left(v_{jx1}\tan\theta - \frac{v_{mp0}B_{z1}}{B_0\cos\theta}\right) \\ &- \Omega_j\frac{B_{z1}}{B_0}\left[-\frac{cE_{x1}}{B_0\sin\theta} + \frac{v_{mp0}}{\Omega_j\sin\theta}\right. \\ &\left.\times\left(\frac{\Gamma_j p_{j0}}{m_j n_{j0}}\frac{1}{v_{mp0}^2} - 1\right)\frac{\partial v_{jx1}}{\partial \xi}\right] - v_{mp0}\frac{\partial v_{jx2}}{\partial \xi} \\ &- \Omega_j v_{jy2}\sin\theta - \Omega_j c\frac{E_{x2}}{B_0} + \frac{1}{m_j n_{j0}}\frac{\partial p_{j2}}{\partial \xi} = 0,\end{aligned} \tag{C13}$$

$$\begin{aligned}&v_{mp0}\frac{\partial}{\partial \xi}\left[-\frac{cE_{x1}}{B_0\sin\theta} + \frac{v_{mp0}}{\Omega_j\sin\theta}\left(\frac{\Gamma_j p_{j0}}{m_j n_{j0}}\frac{1}{v_{mp0}^2} - 1\right)\frac{\partial v_{jx1}}{\partial \xi}\right] \\ &- \Omega_j\frac{B_{z1}}{B_0}v_{jx1} + \Omega_j\frac{c}{B_0}E_{y2} + \Omega_j(v_{jz2}\cos\theta - v_{jx2}\sin\theta) \\ &= 0,\end{aligned} \tag{C14}$$

$$\begin{aligned}&\frac{\partial}{\partial \tau}\left(v_{jx1}\tan\theta - \frac{v_{mp0}B_{z1}}{B_0\cos\theta}\right) \\ &+ v_{jx1}\frac{\partial}{\partial \xi}\left(v_{jx1}\tan\theta - \frac{v_{mp0}B_{z1}}{B_0\cos\theta}\right) - v_{mp0}\frac{\partial v_{jz2}}{\partial \xi} \\ &- \Omega_j\left(\frac{c}{B_0}E_{z2} + \frac{B_{y1}}{B_0}v_{jx1} - v_{jy2}\cos\theta\right) = 0,\end{aligned} \tag{C15}$$

$$\begin{aligned}&\frac{\Gamma_j p_{j0}}{v_{mp0}}\frac{\partial v_{jx1}}{\partial \tau} + \frac{\Gamma_j(\Gamma_j + 1)p_{j0}}{v_{\mathrm{mp0}}}v_{jx1}\frac{\partial v_{jx1}}{\partial \xi} - v_{mp0}\frac{\partial p_{j2}}{\partial \xi} \\ &+ \Gamma_j p_{j0}\frac{\partial v_{jx2}}{\partial \xi} = 0,\end{aligned} \tag{C16}$$

$$\frac{1}{c}\frac{\partial B_{z1}}{\partial \tau} - \frac{v_{mp0}}{c}\frac{\partial B_{z2}}{\partial \xi} + \frac{\partial E_{y2}}{\partial \xi} = 0, \tag{C17}$$

Downloaded 03 Aug 2009 to 133.6.32.19. Redistribution subject to AIP license or copyright; see http://pop.aip.org/pop/copyright.jsp

$$\frac{4\pi}{c}\sum_j n_{j0}q_j\left(v_{jx2}+\frac{1}{v_{mp0}}v_{jx1}^2\right)-\frac{v_{mp0}}{c}\frac{\partial E_{x1}}{\partial \xi}=0, \tag{C18}$$

$$\frac{4\pi}{c}\sum_j n_{j0}q_j\left\{v_{jy2}+\frac{1}{v_{mp0}}v_{jx1}\left[-\frac{cE_{x1}}{B_0\sin\theta}+\frac{v_{mp0}}{\Omega_j\sin\theta}\left(\frac{\Gamma_j p_{j0}}{m_j n_{j0}}\frac{1}{v_{mp0}^2}-1\right)\frac{\partial v_{jx1}}{\partial \xi}\right]\right\}+\frac{v_{mp0}}{c^2}\frac{\partial B_{z1}}{\partial \tau}-\frac{v_{mp0}}{c}\frac{\partial E_{x2}}{\partial \xi}+\frac{\partial B_{z2}}{\partial \xi}=0, \tag{C19}$$

$$\frac{4\pi}{c}\sum_j n_{j0}q_j\left[v_{jz2}+\frac{1}{v_{mp0}}v_{jx1}\left(v_{jx1}\tan\theta-\frac{v_{mp0}B_{z1}}{B_0\cos\theta}\right)\right]+\left(\frac{v_{mp0}^2}{c^2}-1\right)\frac{\partial B_{y1}}{\partial \xi}=0. \tag{C20}$$

Here, by using Eqs. (C3) and (C4), we have eliminated v_{jy1} and v_{jz1}.

To derive the KdV equation, we eliminate higher order quantities, such as, n_{j2} and v_{jx2} from Eqs. (C12)–(C20). We substitute Eq. (C12) in Eq. (C13) to eliminate p_{j2}. From the resultant equation and Eqs. (C14) and (C15), it follows that

$$\begin{aligned}
v_{jy2}=&\frac{\sin\theta}{\Omega_j}\left[1+\frac{c_j^2}{v_{\mathrm{mp0}}^2}(1+\cos^2\theta)\right]\frac{\partial v_{jx1}}{\partial\tau}-\frac{\cos\theta}{\Omega_j}\left(1-\frac{c_j^2}{v_{mp0}^2}\sin^2\theta\right)\times\left[\left(\frac{\partial}{\partial\tau}+v_{jx1}\frac{\partial}{\partial\xi}\right)\left(v_{jx1}\tan\theta-\frac{v_{mp0}B_{z1}}{B_0\cos\theta}\right)\right.\\
&\left.-\Omega_j\left(\frac{c}{B_0}E_{z2}+\frac{B_{y1}}{B_0}v_{jxi}\right)\right]-v_{mp0}\frac{\sin\theta}{\Omega_j}\left(1-\frac{c_j^2}{v_{mp0}^2}\sin^2\theta\right)\frac{\partial}{\partial\xi}\left\{\frac{cE_{x2}}{B_0\sin\theta}-\frac{B_{z1}}{B_0\sin\theta}v_{jx1}-\frac{v_{mp0}}{\Omega_j\sin\theta}\frac{\partial}{\partial\xi}\left[\frac{cE_{x1}}{B_0\sin\theta}\right.\right.\\
&\left.\left.+\frac{v_{mp0}}{\Omega_j\sin\theta}\left(1-\frac{c_j^2}{v_{mp0}^2}\right)\frac{\partial v_{jx1}}{\partial\xi}\right]\right\}-\left(1+\frac{c_j^2}{v_{mp0}^2}\cos^2\theta\right)\frac{cE_{x2}}{B_0}\sin\theta+\left[1+\frac{c_j^2}{v_{mp0}^2}(\Gamma_j+\cos^2\theta)\right]\frac{\sin\theta}{\Omega_j}v_{jx1}\frac{\partial v_{jx1}}{\partial\xi}\\
&+\left(1+\frac{c_j^2}{v_{mp0}^2}\cos^2\theta\right)\frac{B_{y1}\sin\theta}{B_0}\left(v_{jx1}\tan\theta-\frac{v_{mp0}B_{z1}}{B_0\cos\theta}\right),
\end{aligned}\tag{C21}$$

$$\begin{aligned}
\frac{\partial v_{jz2}}{\partial\xi}=&\frac{\sin\theta\cos\theta}{v_{mp0}}\left[1+\frac{c_j^2}{v_{mp0}^2}(1+\cos^2\theta)\right]\frac{\partial v_{jx1}}{\partial\tau}+\frac{v_{mp0}\cos\theta}{\Omega_j}\left(1-\frac{c_j^2}{v_{mp0}^2}\sin^2\theta\right)\frac{\partial^2}{\partial\xi^2}\left[\frac{cE_{x1}}{B_0\sin\theta}+\frac{v_{mp0}}{\Omega_j\sin\theta}\left(1-\frac{c_j^2}{v_{mp0}^2}\right)\frac{\partial v_{jx1}}{\partial\xi}\right]\\
&-\frac{c\cos\theta}{B_0}\left(1-\frac{c_j^2}{v_{mp0}^2}\sin^2\theta\right)\frac{\partial E_{y2}}{\partial\xi}+\frac{B_{z1}\cos\theta}{B_0}\left(1-\frac{c_j^2}{v_{mp0}^2}\sin^2\theta\right)\frac{\partial v_{jx1}}{\partial\xi}+\frac{\cos\theta}{B_0}\left(1-\frac{c_j^2}{v_{mp0}^2}\sin^2\theta\right)\\
&\times\left(B_{z1}\frac{\partial v_{jx1}}{\partial\xi}+v_{jx1}\frac{\partial B_{z1}}{\partial\xi}\right)-\frac{\Omega_j cE_{x2}}{B_0v_{mp0}}\sin\theta\cos\theta\left(1+\frac{c_j^2}{v_{mp0}^2}\cos^2\theta\right)+\frac{\Omega_jB_{z1}cE_{x1}}{B_0^2v_{mp0}}\cos\theta\left(1+\frac{c_j^2}{v_{mp0}^2}\cos^2\theta\right)\\
&-\frac{\Omega_j\sin^2\theta}{B_0v_{mp0}}\left(cE_{z2}+\frac{B_{y1}v_{mp0}B_{z1}}{B_0\sin\theta}\right)\left(1+\frac{c_j^2}{v_{mp0}^2}\cos^2\theta\right)+\left[\left(\frac{\partial}{\partial\tau}+v_{jx1}\frac{\partial}{\partial\xi}\right)\left(v_{jx1}\tan\theta-\frac{v_{mp0}B_{z1}}{B_0\cos\theta}\right)\right]\frac{\sin^2\theta}{v_{mp0}}\\
&\times\left(1+\frac{c_j^2}{v_{mp0}^2}\cos^2\theta\right)+\frac{\sin\theta\cos\theta}{v_{mp0}}\left[1+\frac{c_j^2}{v_{mp0}^2}(\Gamma_j+\cos^2\theta)\right]v_{jx1}\frac{\partial v_{jx1}}{\partial\xi}.
\end{aligned}\tag{C22}$$

Here, we have ignored the terms higher than $\sim c_j^2/v_{mp0}^2$.

We substitute Eqs. (C21) and (C22) in Eqs. (C19) and (C20), respectively, to eliminate v_{jy2} and v_{jz2}. From these equations and Eq. (C17), by eliminating B_{z2}, we have the two equations, from which we eliminate E_{x2} and E_{z2} simultaneously to obtain

$$\begin{aligned}
&\frac{4\pi}{c}\sum_j n_{j0}q_j\left\{2\left(\frac{\sin\theta}{\Omega_j}\frac{c_j^2}{v_{mp0}^2}\right)\frac{\partial v_{jx1}}{\partial\tau}+\frac{v_{mp0}}{B_0\Omega_j}\left(1-\frac{c_j^2}{v_{mp0}^2}\sin^2\theta\right)\frac{\partial B_{z1}}{\partial\tau}+\left[\frac{\sin\theta}{\Omega_j}\left(\frac{c_j^2}{v_{mp0}^2}(1+\Gamma_j)+\frac{1}{\sin^2\theta}\left(\frac{c_j^2}{v_{mp0}^2}-1\right)\right)\right.\right.\\
&\left.-\frac{3\sin\theta}{A}\left(\sum_k n_{k0}q_k\frac{c_k^2}{v_{mp0}^2}\right)\right]v_{jx1}\frac{\partial v_{jx1}}{\partial\xi}+\frac{2v_{mp0}}{B_0\Omega_j}\left(1-\frac{c_j^2}{v_{mp0}^2}\sin^2\theta\right)\frac{\partial B_{z1}v_{jx1}}{\partial\xi}+\frac{v_{mp0}^2}{\Omega_j^2\sin\theta}\frac{\partial^2}{\partial\xi^2}\left[\frac{cE_{x1}}{B_0}+\frac{v_{mp0}}{\Omega_j}\left(1-\frac{c_j^2}{v_{mp0}^2}\right)\frac{\partial v_{jx1}}{\partial\xi}\right]\\
&\times\left(1-\frac{c_j^2}{v_{mp0}^2}\sin^2\theta\right)-\frac{v_{mp0}^2\cos^2\theta}{A\Omega_j\sin\theta}\left(\sum_k n_{k0}q_k\frac{c_k^2}{v_{mp0}^2}\right)\frac{\partial^2}{\partial\xi^2}\left(\frac{cE_{x1}}{B_0}+\frac{v_{mp0}}{\Omega_j}\frac{\partial v_{jx1}}{\partial\xi}\right)+\frac{B_{z1}\cos^2\theta}{B_0^2}\left[\frac{c_j^2}{v_{mp0}^2}-\frac{\Omega_j}{A}\left(\sum_k n_{k0}q_k\frac{c_k^2}{v_{mp0}^2}\right)\right]\\
&\left.\times(cE_{x1}-v_{mp0}B_{y1}\tan\theta)\right\}+\frac{1}{v_{mp0}}\left(\frac{v_{mp0}^2}{c^2}+1\right)\frac{\partial B_{z1}}{\partial\tau}-\frac{v_{mp0}\cos\theta}{A}\left(\sum_k n_{k0}q_k\frac{c_k^2}{v_{mp0}^2}\right)\left(\frac{v_{mp0}^2}{c^2}-1\right)\frac{\partial^2 B_{y1}}{\partial\xi^2}=0,
\end{aligned}\tag{C23}$$

Downloaded 03 Aug 2009 to 133.6.32.19. Redistribution subject to AIP license or copyright; see http://pop.aip.org/pop/copyright.jsp

where the subscript k, as well as j, denotes particle species, and the quantity A is defined as

$$A=\frac{B_0}{4\pi c}\sum_k \omega_{pk}^2\left(1+\frac{c_k^2}{v_{mp0}^2}\cos^2\theta\right). \tag{C24}$$

Since we have ignored the terms of order $(c_j^2/v_{mp0}^2)^2$, the terms related to E_{y2} have vanished.

We have obtained Eq. (C23) by using the y and z components of Ampère's law. Next, we use its x and z components to obtain another different equation. We eliminate v_{jz2} from Eqs. (C20) and (C14), and then eliminate v_{jx2} with the aid of Eq. (C18) to have

$$\begin{aligned}&\frac{4\pi}{c}\sum_j n_{j0}q_j\left\{\frac{v_{mp0}}{\Omega_j\cos\theta}\frac{\partial}{\partial\xi}\left[\frac{cE_{x1}}{B_0\sin\theta}+\frac{v_{mp0}}{\Omega_j\sin\theta}\right.\right.\\&\quad\left.\left.\times\left(1-\frac{c_j^2}{v_{mp0}^2}\right)\frac{\partial v_{jx1}}{\partial\xi}\right]\right\}+\left(\frac{v_{mp0}^2}{c^2}-1\right)\frac{\partial B_{y1}}{\partial\xi}\\&\quad+\frac{v_{mp0}}{c}\tan\theta\frac{\partial E_{x1}}{\partial\xi}=0,\end{aligned} \tag{C25}$$

which, by virtue of Eq. (A7), becomes

$$\begin{aligned}&\frac{v_{mp0}}{c}\left(\frac{c^2}{v_A^2}+\sin^2\theta\right)E_{x1}+\left(\frac{v_{mp0}^2}{c^2}-1\right)\sin\theta\cos\theta B_{y1}\\&\quad+\frac{B_0v_{mp0}^2}{c^2}\sum_j\left[\frac{\omega_{pj}^2}{\Omega_j^3}\left(1-\frac{c_j^2}{v_{mp0}^2}\right)\frac{\partial v_{jx1}}{\partial\xi}\right]=0.\end{aligned} \tag{C26}$$

3. Lowest order quantities and the KdV equation

Now we express all the lowest order quantities in terms of B_{z1}. From Eqs. (C3)–(C5), we have

$$\begin{aligned}\frac{\partial v_{jx1}}{\partial\xi}=&-\frac{c\Omega_j}{v_{\mathrm{mp}0}B_0}\cos\theta\left(1+\frac{c_j^2}{v_{mp0}^2}\cos^2\theta\right)(E_{x1}\cos\theta\\&+E_{z1}\sin\theta)+\frac{v_{mp0}}{B_0}\sin\theta\left(1+\frac{c_j^2}{v_{mp0}^2}\cos^2\theta\right)\frac{\partial B_{z1}}{\partial\xi}.\end{aligned} \tag{C27}$$

By substituting Eq. (C27) in Eq. (C9), we obtain

$$E_{x1}\cos\theta+E_{z1}\sin\theta\simeq\frac{1}{c}\frac{\Sigma_j(\omega_{pj}^2/\Omega_j)c_j^2}{\omega_p^2}\sin\theta\cos\theta\frac{\partial B_{z1}}{\partial\xi}. \tag{C28}$$

We substitute Eq. (C27) in Eq. (C26). Then, with the aid of Eqs. (A7), (A10), and (C7), it follows that

$$\begin{aligned}&\frac{v_{mp0}}{c}\left[\frac{c^2}{v_A^2}\sin^2\theta\left(1+\frac{c_s^2}{v_{mp0}^2}\cos^2\theta\right)+\sin^2\theta\right]E_{x1}\\&\quad+\frac{v_{mp0}}{c}\left[\left(\frac{c^2}{v_{mp0}^2}-1\right)-\frac{c^2}{v_A^2}\left(1-\frac{c_s^2}{v_{mp0}^2}\right)\right]\\&\quad\times\sin\theta\cos\theta E_{z1}+\frac{v_{\mathrm{mp}0}^3}{c^2}\\&\quad\times\sin\theta\sum_j\left[\frac{\omega_{pj}^2}{\Omega_j^3}\left(1-\frac{c_j^2}{v_{mp0}^2}\right)\right]\frac{\partial B_{z1}}{\partial\xi}=0.\end{aligned} \tag{C29}$$

From (C28) and (C29), we have

$$E_{x1}=-\left(\frac{v_A^2}{v_A^2+c_s^2}\right)\frac{v_{mp0}^4}{c^3\sin\theta}\sum_j\frac{\omega_{pj}^2}{\Omega_j^3}\left(1-\frac{c_j^2}{v_{mp0}^2}\sin^2\theta\right)\frac{\partial B_{z1}}{\partial\xi}, \tag{C30}$$

$$\begin{aligned}E_{z1}=&\left[\left(\frac{v_A^2}{v_A^2+c_s^2}\right)\frac{v_{mp0}^4\cos\theta}{c^3\sin^2\theta}\sum_j\frac{\omega_{pj}^2}{\Omega_j^3}\left(1-\frac{c_j^2}{v_{mp0}^2}\sin^2\theta\right)\right.\\&\left.+\frac{1}{c}\frac{\Sigma_j(\omega_{pj}^2/\Omega_j)c_j^2}{\omega_p^2}\cos\theta\right]\frac{\partial B_{z1}}{\partial\xi}.\end{aligned} \tag{C31}$$

Also, from Eqs. (C27) and (C28), we find v_{jx1} as

$$\begin{aligned}v_{jx1}=v_{mp0}&\left[-\frac{\Omega_j}{v_{mp0}^2}\frac{\Sigma_j(\omega_{pj}^2/\Omega_j)c_j^2}{\omega_p^2}\sin\theta\cos^2\theta\right.\\&\left.+\sin\theta\left(1+\frac{c_j^2}{v_{mp0}^2}\cos^2\theta\right)\right]\frac{B_{z1}}{B_0}.\end{aligned} \tag{C32}$$

Substituting Eq. (C32) in Eqs. (C2), (C4), and (C6), we obtain, respectively,

$$\begin{aligned}n_{j1}=n_{j0}&\left[-\frac{\Omega_j}{v_{mp0}^2}\frac{\Sigma_j(\omega_{pj}^2/\Omega_j)c_j^2}{\omega_p^2}\sin\theta\cos^2\theta\right.\\&\left.+\sin\theta\left(1+\frac{c_j^2}{v_{mp0}^2}\cos^2\theta\right)\right]\frac{B_{z1}}{B_0},\end{aligned} \tag{C33}$$

$$\begin{aligned}v_{jz1}=v_{mp0}&\left[-\frac{\Omega_j}{v_{mp0}^2}\frac{\Sigma_j(\omega_{pj}^2/\Omega_j)c_j^2}{\omega_p^2}\sin^2\theta\cos\theta\right.\\&\left.+\frac{\sin^2\theta}{\cos\theta}\left(1+\frac{c_j^2}{v_{mp0}^2}\cos^2\theta\right)-\frac{1}{\cos\theta}\right]\frac{B_{z1}}{B_0},\end{aligned} \tag{C34}$$

$$\begin{aligned}p_{j1}=\Gamma_jp_{j0}&\left[-\frac{\Omega_j}{v_{mp0}^2}\frac{\Sigma_j(\omega_{pj}^2/\Omega_j)c_j^2}{\omega_p^2}\sin\theta\cos^2\theta\right.\\&\left.+\sin\theta\left(1+\frac{c_j^2}{v_{mp0}^2}\cos^2\theta\right)\right]\frac{B_{z1}}{B_0}.\end{aligned} \tag{C35}$$

With the help of Eqs. (C30) and (C32), Eq. (C3) becomes

Downloaded 03 Aug 2009 to 133.6.32.19. Redistribution subject to AIP license or copyright; see http://pop.aip.org/pop/copyright.jsp

$$v_{jy1} = \left\{ \left(\frac{v_A^2}{v_A^2 + c_s^2} \right) \frac{v_{mp0}^4}{B_0 c^2 \sin^2 \theta} \sum_j \frac{\omega_{pj}^2}{\Omega_j^3} \left(1 - \frac{c_j^2}{v_{mp0}^2} \sin^2 \theta \right) + \left(\frac{c_j^2}{v_{mp0}^2} - 1 \right) \left[- \frac{1}{B_0} \frac{\Sigma_j (\omega_{pj}^2/\Omega_j) c_j^2}{\omega_p^2} \cos^2 \theta + \frac{v_{mp0}^2}{B_0 \Omega_j} \left(1 + \frac{c_j^2}{v_{mp0}^2} \cos^2 \theta \right) \right] \right\} \frac{\partial B_{z1}}{\partial \xi}. \quad \text{(C36)}$$

From Eqs. (C7) and (C31), we find that

$$B_{y1} = - \left[\left(\frac{v_A^2}{v_A^2 + c_s^2} \right) \frac{v_{mp0}^3 \cos \theta}{c^2 \sin^2 \theta} \sum_j \frac{\omega_{pj}^2}{\Omega_j^3} \left(1 - \frac{c_j^2}{v_{mp0}^2} \sin^2 \theta \right) + \frac{1}{v_{mp0}} \frac{\Sigma_j (\omega_{pj}^2/\Omega_j) c_j^2}{\omega_p^2} \cos \theta \right] \frac{\partial B_{z1}}{\partial \xi}. \quad \text{(C37)}$$

If we substitute the lowest order quantities expressed in terms of B_{z1} in Eq. (C23), then, using Eqs. (10), (A7), and (A10), we obtain the KdV equation (35).

APPENDIX D: PARALLEL ELECTRIC FIELD IN THE COLD PLASMA LIMIT

By calculating up to the second lowest order terms, we obtain the parallel electric field in a cold plasma.

For $T_j = 0$, with the aid of Eqs. (C28), (C30), and (C32), we find that

$$E_{x1} \cos \theta + E_{z1} \sin \theta = 0, \quad \text{(D1)}$$

$$E_{x1} = - \frac{\tilde{v}_A^4}{c^3 \sin \theta} \sum_j \frac{\omega_{pj}^2}{\Omega_j^3} \frac{\partial B_{z1}}{\partial \xi}, \quad \text{(D2)}$$

$$v_{jx1} = \tilde{v}_A \frac{B_{z1}}{B_0} \sin \theta, \quad \text{(D3)}$$

and with the use of Eqs. (C7) and (D1), Eq. (C13) reduces to

$$\frac{\partial v_{jx1}}{\partial \tau} - \tilde{v}_A \frac{\partial v_{jx2}}{\partial \xi} + \left(v_{jx1} + \frac{\tilde{v}_A B_{z1}}{B_0 \sin \theta} \right) \frac{\partial v_{jx1}}{\partial \xi} + \Omega_j \left(\frac{B_{y1}}{B_0} v_{jx1} \tan \theta - v_{jy2} \sin \theta - \frac{c E_{x2}}{B_0} \right) = 0. \quad \text{(D4)}$$

Since, as Eq. (D3) shows, v_{jx1} is independent of particle species, we obtain from Eqs. (C18) and (C20)

$$\sum_j n_{j0} q_j v_{jx2} = \frac{\tilde{v}_A}{4\pi} \frac{\partial E_{x1}}{\partial \xi}, \quad \text{(D5)}$$

$$\sum_j n_{j0} q_j v_{jz2} = \frac{\tilde{v}_A}{4\pi \tan \theta} \left(\frac{c^2}{\tilde{v}_A^2} - 1 \right) \frac{\partial E_{x1}}{\partial \xi}, \quad \text{(D6)}$$

where use has been made of the relations (C7) and (D1).

We multiply Eq. (D4) by $n_{j0} q_j$ and sum over particle species j. Then, substituting Eq. (D5) for v_{jx2} yields

$$- \frac{\tilde{v}_A^2}{4\pi} \frac{\partial^2 E_{x1}}{\partial \xi^2} + \sum_j n_{j0} q_j \Omega_j \times \left(\frac{B_{y1}}{B_0} v_{jx1} \tan \theta - v_{jy2} \sin \theta - \frac{c E_{x2}}{B_0} \right) = 0. \quad \text{(D7)}$$

Similarly, from Eqs. (C15) and (D6), it follows that

$$\frac{\tilde{v}_A^2}{4\pi \tan \theta} \left(1 - \frac{c^2}{\tilde{v}_A^2} \right) \frac{\partial^2 E_{x1}}{\partial \xi^2} - \sum_j n_{j0} q_j \Omega_j \left(\frac{B_{y1}}{B_0} v_{jx1} - v_{jy2} \cos \theta + \frac{c E_{z2}}{B_0} \right) = 0. \quad \text{(D8)}$$

Combining Eqs. (D2), (D7), and (D8), we find the parallel electric field (44) in the cold plasma limit.

[1] H. Alfvén and C.-G. Fälthammer, *Cosmical Electrodynamics* (Clarendon, Oxford, 1963).
[2] D. Biskamp, *Magnetic Reconnection in Plasmas* (Cambridge University Press, Cambridge, 2000).
[3] J. V. Hollweg, Astrophys. J. **277**, 392 (1984).
[4] N. Bessho and Y. Ohsawa, Phys. Plasmas **6**, 3076 (1999); **9**, 979 (2002).
[5] S. Takahashi and Y. Ohsawa, Phys. Plasmas **14**, 112305 (2007).
[6] H. Hasegawa, S. Usami, and Y. Ohsawa, Phys. Plasmas **10**, 3455 (2003); H. Hasegawa, K. Kato, and Y. Ohsawa, *ibid.* **12**, 082306 (2005).
[7] P. A. Sturrock, Astrophys. J. **164**, 529 (1971).
[8] C. F. Kennel and R. Pellat, J. Plasma Phys. **15**, 335 (1976).
[9] J.-I. Sakai and T. Kawata, J. Phys. Soc. Jpn. **49**, 753 (1980).
[10] J. N. Leboeuf, M. Ashour-Abdalla, T. Tajima, C. F. Kennel, F. V. Coroniti, and J. M. Dawson, Phys. Rev. A **25**, 25 (1982).
[11] G. S. Lakhina and F. Verheest, Astrophys. Space Sci. **253**, 97 (1997).
[12] G. A. Stewart and E. W. Laing, J. Plasma Phys. **47**, 295 (1992).
[13] C. S. Reynolds, A. C. Fabian, A. Celotti, and M. J. Rees, Mon. Not. R. Astron. Soc. **283**, 873 (1996).
[14] K. Hirotani, S. Iguchi, M. Kimura, and K. Wajima, Publ. Astron. Soc. Jpn. **51**, 263 (1999).
[15] Y. A. Gallant, M. Hoshino, A. B. Langdon, J. Arons, and C. E. Max, Astrophys. J. **391**, 73 (1992).
[16] V. I. Berezhiani and S. M. Mahajan, Phys. Rev. Lett. **73**, 1110 (1994).
[17] H. Hasegawa, S. Irie, S. Usami, and Y. Ohsawa, Phys. Plasmas **9**, 2549 (2002).
[18] T. Kakutani, H. Ono, T. Taniuti, and C. C. Wei, J. Phys. Soc. Jpn. **24**, 1159 (1968).
[19] T. Kakutani and H. Ono, J. Phys. Soc. Jpn. **26**, 1305 (1969).
[20] Y. Ohsawa, Phys. Fluids **29**, 1844 (1986).
[21] C. S. Gardner and G. K. Morikawa, Commun. Pure Appl. Math. **18**, 35 (1965).
[22] H. Washimi and T. Taniuti, Phys. Rev. Lett. **17**, 996 (1966).
[23] P. C. Liewer, A. T. Lin, J. M. Dawson, and M. Z. Caponi, Phys. Fluids **24**, 1364 (1981).
[24] A. B. Langdon and C. K. Birdsall, Phys. Fluids **13**, 2115 (1970).
[25] T. Kawashima, S. Miyahara, and Y. Ohsawa, J. Phys. Soc. Jpn. **72**, 1664 (2003).
[26] Y. Ohsawa, Phys. Fluids **29**, 2474 (1986).

Downloaded 03 Aug 2009 to 133.6.32.19. Redistribution subject to AIP license or copyright; see http://pop.aip.org/pop/copyright.jsp